UNIVERSITY OF MICHIGAN

NERS/BIOE 481

Lecture 11 A
Computed Tomography (CT)

Michael Flynn, Adjunct Prof
Nuclear Engr & Rad. Science
mikef@umich.edu
mikef@rad.hfh.edu

Henry Ford Health System
RADIOLOGY RESEARCH

A) X-ray Computed Tomography …(L11)
B) CT Reconstruction Methods …(L11/L12)

A) X-ray Computed Tomography
1. Basic Concepts (2 slides)
2. Historical Developments
3. X-ray Source
4. Detectors
5. Multi-slice scanners
6. Recent Advances
7. Cone beam systems
8. Tomosynthesis systems

From Lecture 05

$$P(r,\theta) = -\ln\left(\frac{\varphi}{\varphi_o}\right) = \int_0^T \mu(t)dt$$

- The argument of the exponential factor describing the attenuation through an object path is known as the Radon transform.
- It's form is that of a generalized pathlength integral of a density function.
- The inverse solution to the Radon transform, i.e. $\mu(x,y)$ as a function of $P(r,\theta)$, is used in computed tomography.

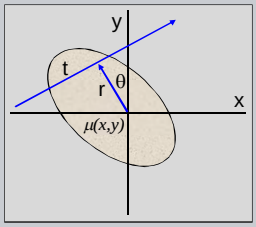

In the Radon transform equation above, the attenuation shown as a function of the projection path variable, $\mu(t)$, is more formally written as $\mu(r,\theta)$ or $\mu(x,y)$

The line integral of $\mu(t)$, $P(r,\theta)$, is referred to a a 'Projection Value'.
The set of all values obtained in one exposure is called a 'Projection View.

- CT image reconstruction seeks a solution for the material properties of an object, $\mu(x,y)$, based on projections measurements, $P(r,\theta)$, taken at many positions and orientations as indicated by r and θ.
- In 1917, Radon proved that a solution exists if $P(r,\theta)$ is known for all values of r and θ.
- Practical numeric methods to solve this problem were not developed until 50 years later.

A) X-ray Computed Tomography
1. Basic Concepts
2. Historical Developments (16 slides)
3. X-ray Source
4. Detectors
5. Multi-slice scanners
6. Recent Advances
7. Cone beam systems
8. Tomosynthesis systems

Early CT History

- 1917
  Radon's theory of image reconstruction from projections
- 1956
  Bracewell constructed solar map from projection data
- 1961, 1963
  Oldendorf, Cormack developed Laboratory CT devices
- 1968
  Kuhl & Edwards developed nuclear imaging emission tomography device (SPECT).
- 1972
  Godfrey Hounsfield and the Central Research Laboratory of EMI, Ltd complete the development of a medical CT device for scanning the human head.

EMI Laboratory Device

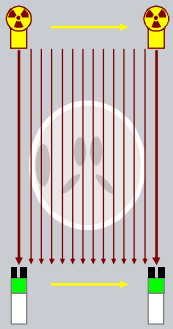

1st Generation Translate – Rotate Geometry

- A pencil beam of radiation is scanned linearly across the subject to acquire a set of parallel projections.

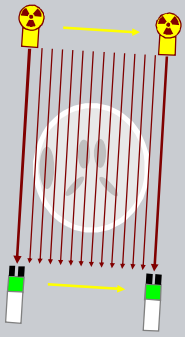

1st Generation Translate – Rotate Geometry

- The gantry is rotated slightly and the linear scan repeated.

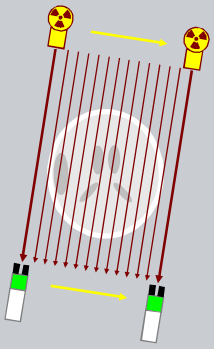

1st Generation Translate – Rotate Geometry

- A large number of translate scans is performed with small angle changes
- Completion of a scan for a single slice required about 5 minutes.

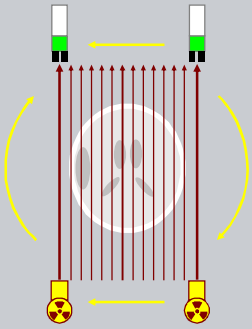

1st Generation Translate – Rotate Geometry

- The last translation scan is obtained at 180 degrees of rotation relative to the first translation.
- The 1st generation geometry was used in early EMI head and body scanners and devices built by Neuroscan and Pfizer

From Lecture 01

1973
First commercially available clinical CT head scanner on market (EMI)

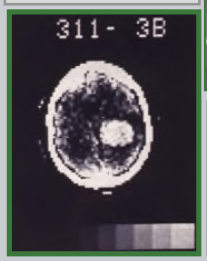

- One of the first EMI head CT scanners in the US was installed at Henry Ford Hospital (Detroit, MI) in 1973.
- The CT image shown to the left was obtained at the Cleveland Clinic in 1974. A large meningioma has been enhanced by iodinated contrast material.

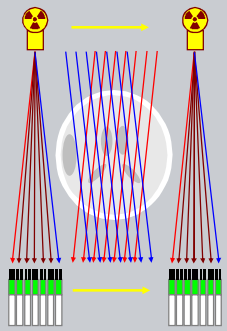

2nd Generation
Translate – Rotate

- A set of radiation beams arrange in a fan geometry is scanned linearly across the subject.
- This allows multiple sets of parallel beam projections to be acquired at the same time

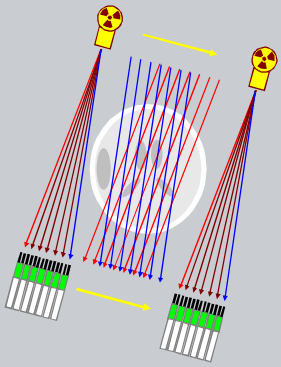

2nd Generation
Translate – Rotate

- A relatively large rotation step is made and the translation scan repeated.
- This approach was used in 1975 by Technicare and then by EMI for head and body scanners.
- Scan times were reduced to 2 minutes and eventually 20 secs.

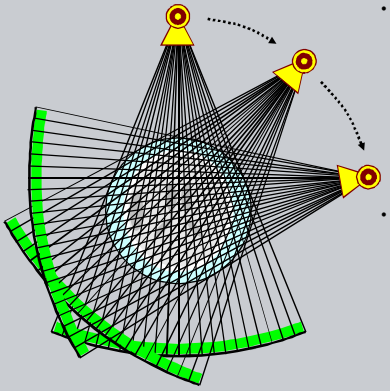

- In 1976, devices were introduced for which the number of detectors and the width of the fan allowed the scan circle to be fully measured with one x-ray pulse.
- Simple rotation of the x-ray tube and detector assembly provided all measurements needed for image reconstruction.

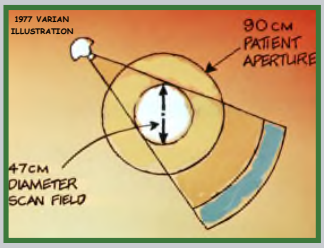

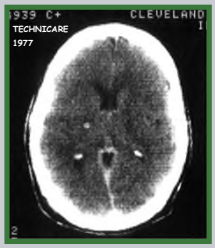

- Improved detectors and scanning mechanisms led to rotating fan beam devices in 1976 with 5 sec scan times.
- In the next two years, systems were sold by GE, Varian, Searle, Technicare, and Siemens. This design is still employed in modern medical CT scanners.
- Since each detector element tracks a circle, careful calibration is needed to avoid ring artifacts.

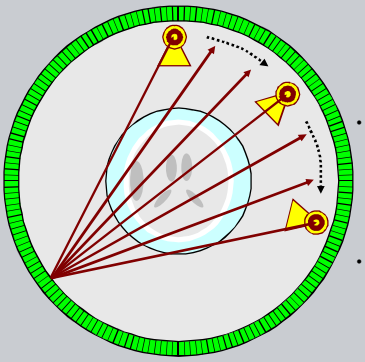

- In 1977, devices with a fixed ring of detectors and a rotating x-ray tube were introduced by AS&E (Pfizer) and Picker.
- These devices were not susceptible to detector fluctuation artifacts (ring) and were adopted by other companies .
- A single detector acquires a fan beam of projections as the x-ray tube rotates past the scan circle.

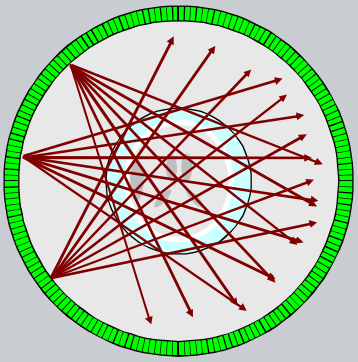

- The signals acquired by all detectors form a set of rotating fan beams similar to than acquired with 3rd generation systems.
- Because the approach requires more detectors, the 4th generation approach has not be used to date for multi-slice scanners.

VII.A.2 – 1985 - dose limited performance

- Detection Efficiency & Dose:
  If x-rays are detected efficiently, the image noise associated with a specific pixel size and slice thickness is limited by the amount of radiation energy deposited in the patient.
- Image Quality:
  The resolution and noise of medical CT images has improved only modestly since 1985.
- Speed:
  However, the acquisition speed has improved dramatically.

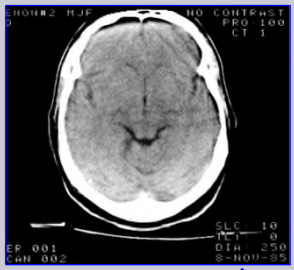

1985

VII.A.2 – 1990 – spiral/helical scanning

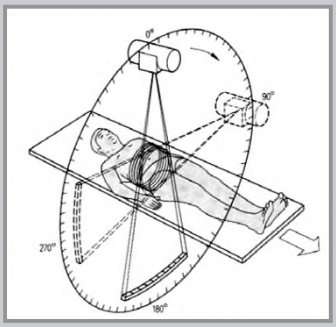

Continuous scanning was introduced in 1990 using slip-ring technology for electronic interface to the detector and x-ray tube and continuous motion of the patient table.

The 3rd generation geometry was adopted for helical/spiral devices and eventually extended to the modern multislice scanner.

VII.A.2 – 1990 – spiral/helical scanning

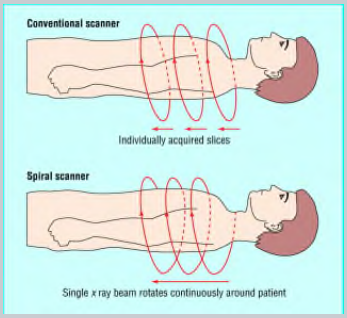

These systems were labeled as either:

- *spiral* (Siemens)

or

- *helical* (GE)

because of the motion of the tube-detector relative to the patient.

In 1990, the Siemens Somatom Plus-S achieved 32 second continuous spiral scan with constant tabletop feed. Subsecond (.75 s) rotation speed was achieved in 1994 with the Somatom Plus 4.

VII.A.2 – 2000 - Increased Volumes

The amount of image data acquired increased 6X from 1990 to 2000 due to:

- Helical/Spiral scan geometry
- Improved reconstruction time
- Improved X-ray tube heat capacity

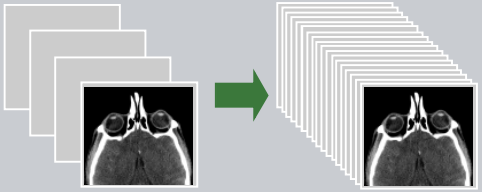

1990	2000
25 cm scan length	25 cm scan length
10.0 mm thick scans	1.25 mm thick scans
25 slices	150 slices

VII.A – CT outline

A) X-ray Computed Tomography

1. Basic Concepts
2. Historical Developments
3. X-ray Source (7 slides)
4. Detectors
5. Multi-slice scanners
6. Recent Advances
7. Cone beam systems
8. Tomosynthesis systems

VII.A.3 – Tube Capacity and scan time

- Modern CT tubes exceed 7-8 MHU with cooling rates of 1.4 MHU/min.
- Typical technique is 120-140 kVp, 100-400 mA-s (.1 to .5 MHU/sec)
- Tube heat capacity may limit the scan time in one run. A time delay is then required before the next scan is started.

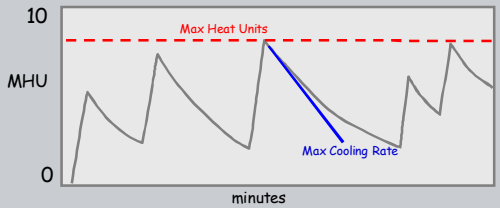

- Multi-slice scanners complete a full scan more quickly and thus produce less heat loading than single slice scanners.

1 Heat Unit (HU) = 1 Joule V x A = Watts = HU/sec

VII.A.3 – CT X-Ray Generator & Heat Exchanger

Modern scanners with continuous rotation use high power tubes with fast rotation time.

GE Performix HD Tube
Up to 680 mA on the small focal spot

The high heat load of CT xray sources requires oil coolant circulation and heat exchanger units.

VII.A.3 – Cooled Anode x-ray tube.

From Lecture 03

One manufacturer (Siemens) uses an x-ray tube where the entire tube body rotates, rather than just the anode, as is the case with conventional designs. This change allows all the bearings to be located outside the evacuated tube, and enables the anode to be cooled more efficiently.

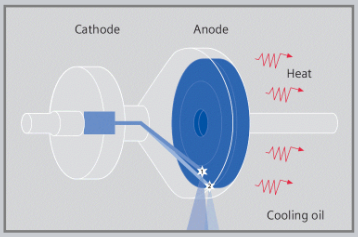

- The Straton has a low inherent heat capacity of 0.8 MHU, but an extremely fast cooling rate of 5 MHU/min (83 kHU/sec).
- This permits continuous scanning with no time limit at 120 kVp and 700 mA.

VII.A.3 – X-ray Beam Collimation

- X-rays are collimated to a fan beam using collimating shutters place before and after the patient.
- The post patient collimator provides a more well defined beam profile in the Z direction but removes radiation signals that have exposed the patient.

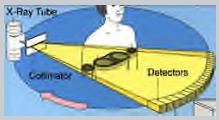

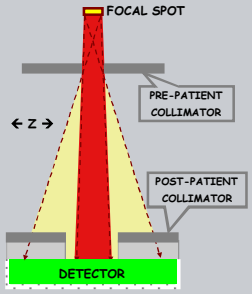

VII.A.3 – Beam Shaping (Bow-tie) Filter

- Beam shaping (Bow-tie) filters provide a more constant signal to all detector elements.
- X-ray spectral shape is kept similar which reduces artifacts.
- Radiation dose at the patient surface is reduced.

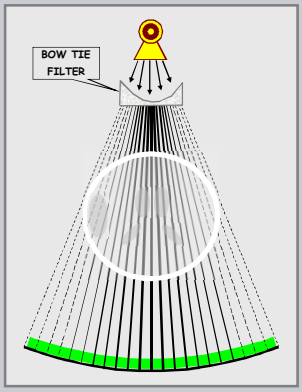

VII.A.3 – Dynamic Flux Control (DFC)

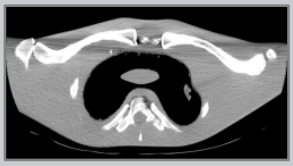

- DFC reduces mA when the x-ray attenuation is low.
- mA is increased when the attenuation is high.
- 1985: Developed using sinusoidal variation in mA.

Toth,Technicare, US5400378.

If mA is constant during rotation, thick regions are underpenetrated and have excess noise.

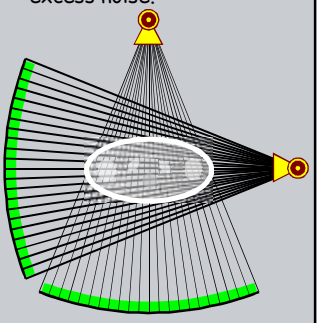

VII.A.3 – Dynamic Flux Control

Kalendar et.al., Physica Medica 24, 2008

Advanced systems now automatically monitor transmission versus rotation and dynamically adjust mA.

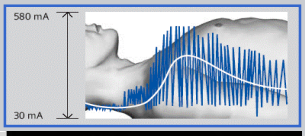

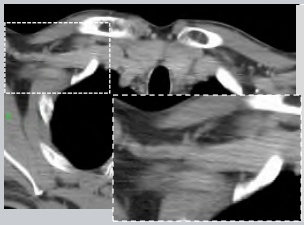

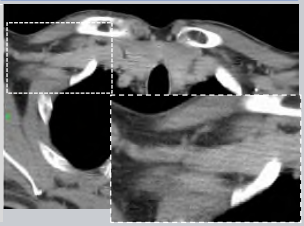

Conventional Scan, 327 mA-S

Under penetration causes excessive noise and anisotropic noise texture.

mA modulation, 166 mA-S avg.

Dynamic flux control reduces noise and streak artifacts.

VII.A – CT outline

A) X-ray Computed Tomography

1. Basic Concepts
2. Historical Developments
3. X-ray Source
4. Detectors (7 slides)
5. Multi-slice scanners
6. Recent Advances
7. Cone beam system
8. Tomosynthesis systems

VII.A.4 – Xenon Ionization Detectors

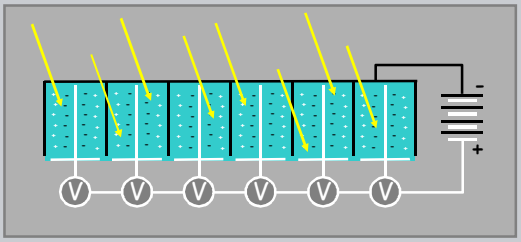

- The ionization of high-pressure zenon gas molecules produces ions (+) and electrons (-) that migrate to oppositely charged collection plates. The current produced is converted to a voltage that is proportional to the rate at which radiation energy is absorbed.
- These detectors were used for early fan beam systems such as the GE 7800, 8800, and 9800 systems made from 1975 to 1985.

VII.A.4 – Solid Scintillation Detectors

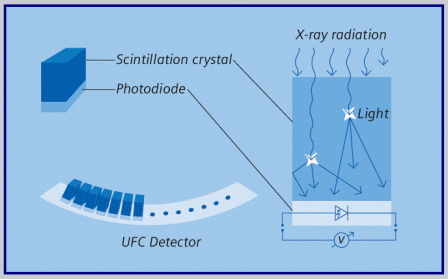

For single slice scanners, each detector element is long relative to the magnified Z width of the fan beam. X-rays from the entire beam width are integrated for any slice width

- X-rays absorbed in the scintillation material produce light in proportion to the amount of energy deposited.
- This light is detected by a photodiode and converted to a voltage level by a preamplifier.

VII.A.4 – Scintillator-photodiode detectors

- Most systems made later than ~1988 have used scintillator photodiode detectors.
- Early systems used:
  - Bismuth Germanate (BGO),
  - Gadolinium OxySulfide (Gd_2O_2W),
  - Cadmium Tungstate ($CdWO_4$).
- Recent designs have used ceramic scintillators made from yttrium/lutetium oxides and europium oxides with rare earth impurities that produce very fast response with little afterglow. (GE HiLight, Siemens UFC).

Terbium or Lutetium doped Garnet phosphors have been recently developed (GE). These have high light output, low afterglow, short decay time, and high x-ray stopping power.

VII.A.4 – CT detector after-glow

- Primary decay time constant, α_1, is for fast $e^{-t/\alpha 1}$ decay.
- Typical scan times are 1000 times the primary decay time

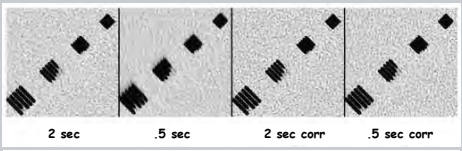

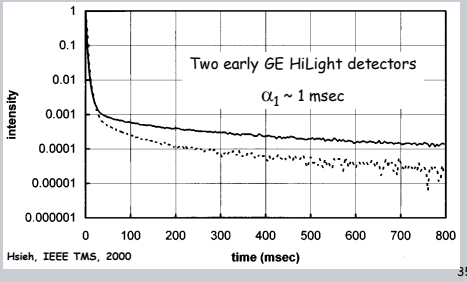

VII.A.4 – Multi-slice Detectors

- Detectors with multiple elements in the Z direction were introduced in 1998.
- Helical scans done with multiple element detectors provide thinner slices for the same x-ray beam width.
- Alternatively, faster table motion can be used with a thicker x-ray beam to obtain the same slice width as for a single detector scan.

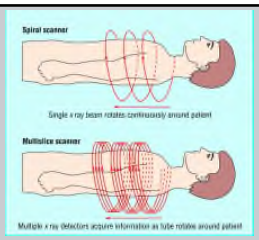

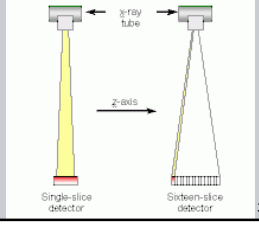

VII.A.4 – Multi-slice Detectors

The current generation of CT scanners uses large area detectors with modular design.

Broad fan beams increase scattered radiation.

Anti-scatter grids can improve contrast.

Media link for Philips CT detector

VII.A.4 – Multi-slice Detectors

Current detector modules have reduced noise resulting in improved performance for low mA techniques.

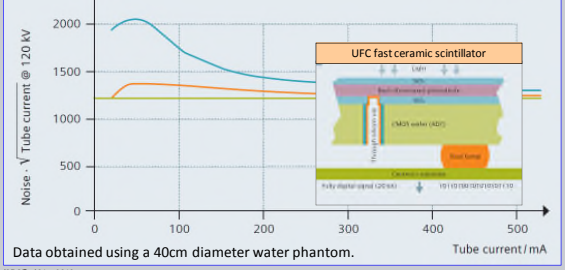

Data obtained using a 40cm diameter water phantom.

VII.A – CT outline

A) X-ray Computed Tomography

1. Basic Concepts
2. Historical Developments
3. X-ray Source
4. Detectors
5. Multi-slice scanners (9 slides)
6. Recent Advances
7. Cone beam systems
8. Tomosynthesis systems

VII.A.5 – Helical CT Pitch

- In modern scanners, the x-ray tube and detector rotate continuously with slip ring bearings as the table moves with velocity, v_t.
- The width of the x-ray beam at the rotation center, B_w, is illustrated in Fig-B for a 360 degree rotation.
- The subject moved about twice the beam width during this rotation.
- The scan pitch is defined as (table travel / beam width);

$$P = (v_t * t_r) / B_w$$

P = *Pitch*
v_t = *table velocity*
t_r = *rotation time*
B_w = *beam width*

A

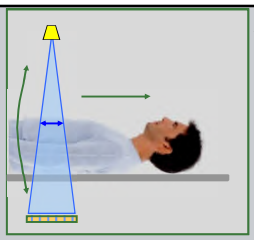

B

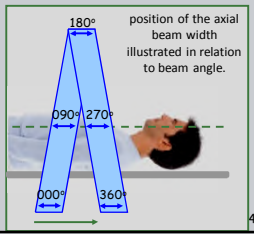

VII.A.5 – Helical CT Pitch

- Measurements should be made from all directions for each point in the region of reconstruction.
- A pitch of 2 leaves portions of the subject incompletely sampled.
- A pitch of 1.0 provides some redundant sampling.
- Pitch values of about 1.1 – 1.3 are common.

$$P = (v_t * t_r) / B_w$$

P = *Pitch*
v_t = *table velocity*
t_r = *rotation time*
B_w = *beam width*

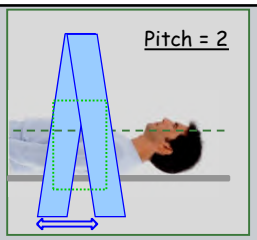

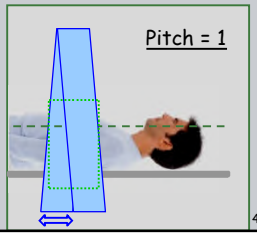

VII.A.5 – Helical CT beam width

- The detector elements for the projections through a point in the object depend on the detector rotation because of the table movement.
- The width of a reconstructed slice is determined by the reconstruction region considered rather than by collimation.

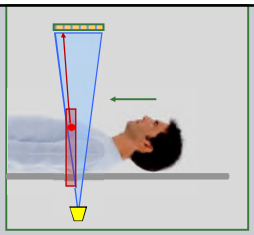

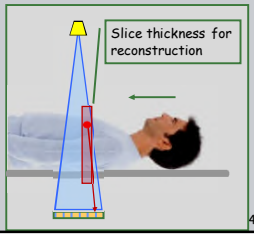

VII.A.5 – Helical CT – slice width and position

- The CT image has a slice width and position determined by the reconstruction.
- Slice intervals that overlap the slice width provide improved object sampling.
- Thin overlapped slices are used for coronal and sagittal views and for 3D surface renderings.

Note: The slice positions in this figure have been displaced vertically to illustrate the overlap of the slice widths.

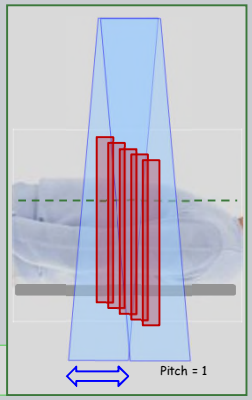

VII.A.5 – Evolution of Multislice Scanners

Multi-slice CT technology developed rapidly from 2000 - 2010

• 1999	4 slice	20 mm	.70-.80 sec
• 2002	16 slice	20 mm	.40-.50 sec
• 2005	64 slice	40 mm	.35-.40 sec
• 2008	256+ slice	80+ mm	< .30 sec

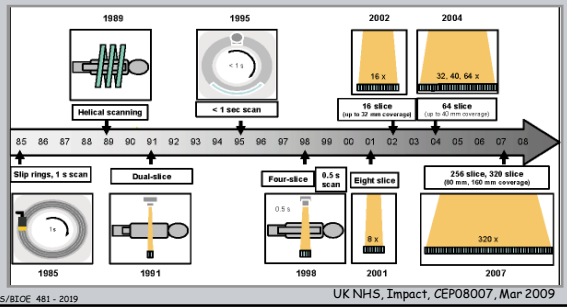

UK NHS, Impact, CEP08007, Mar 2009

VII.A.5 – 64 slice CT scanners

64 slice scanners, c. 2006

Scanner	Data Channels (# x mm)	Detector Z Length (mm)	Rotation Speed (sec)
GE LightSpeed VCT	64 x 0.625	40	0.35
Philips Brilliance 64	64 x 0.625	40	0.40
Siemens Sensation 64	64 x 0.6* 24 x 1.2	28.8	0.37 (.33 opt.)
Toshiba Aquilion 64	64 x 0.5	32	0.40

* 64 x 0.6 mm data channels achieved using 32 x 0.6 mm detectors and z-axis flying focal spot

VII.A.5 – 128+ slice CT scanners

128 – 320 slice CT scanners, c. 2010

Scanner	Data Channels	Z Length (mm)	Rotation Speed (sec)
GE CT750 HD	128	40	0.35
Philips Brilliance iCT	128	80	0.33
Siemens Definition AS*	128	38	0.30
Toshiba Aquilion ONE	320	160	0.35

* 128 data channels achieved using 64 detectors and z-axis flying focal spot

VII.A.5 – 128 slice CT scanner

GE CT750 HD

Media link on rotation

VII.A.5 – Multi-Slice Applications

Multi-slice technology has led to:

- Increased use of CT angiography.
- Thin slice lung scans with single breath hold.
- Whole body scans and increased utilization for trauma evaluation.
- Increased use of 3D image analysis.
- Cardiac dynamic imaging.

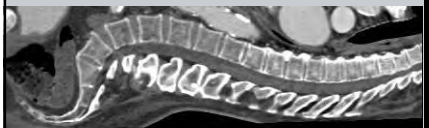

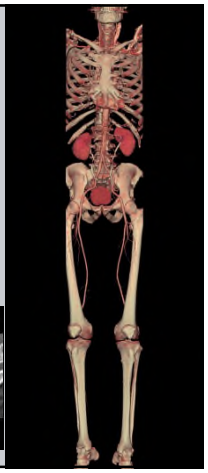

A) X-ray Computed Tomography

1. Basic Concepts
2. Historical Developments
3. X-ray Source
4. Detectors
5. Multi-slice scanners
6. Recent Advances (15 slides)
7. Cone beam systems
8. Tomosynthesis systems

2014 – GE Revolution CT

Gemstone Clarity detector (garnet)

NEW INTEGRATED MODULE

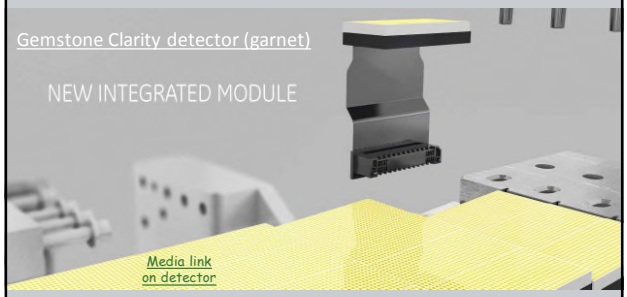

Media link on detector

256 data channels
- 0.625 mm row thickness
- 160 mm Z coverage

Note: @ rotation center

Improved center mount design
- 0.28 sec rotation time
- 0.20 sec gantry rating

4/2014 FDA approval

Siemens Dual Source CT scanners

2012 -Somatom Definition Flash

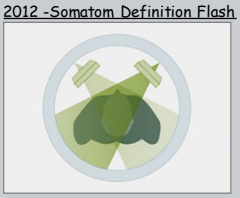

2014 -Somatom Force

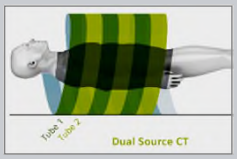

Detector	2 x Stellar detector
Number of slices	256 (2 x 128)
Rotation time	0.28 s^{-1}
Temporal resolution	75 ms
Generator power	200 kW (2 x 100 kW)
kV steps	70, 80, 100, 120, 140 kV
Isotropic resolution	0.33 mm
Max. scan speed	458 mm/s^{-1} with Flash Spiral

Detector	2 x Stellar^{Infinity} detector with 3D Anti-Scatter collimator
Channels	384 (2 x 192)
Rotation time	up to 0.25 s
Temporal resolution	66 ms
Generator power	240 kW (2 x 120 kW)
kV settings	70-150 kV, in steps of 10
Spatial resolution	0.24 mm
Max. scan speed	737 mm/s^{-1} with Turbo Flash

Dual Energy CT

Dual source CT systems that set kV and filtration differently on each source provide high quality material specific images.

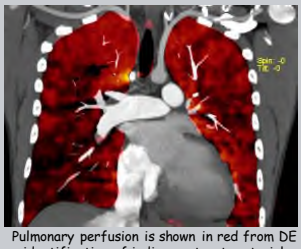

Pulmonary perfusion is shown in red from DE identification of iodine contrast material.

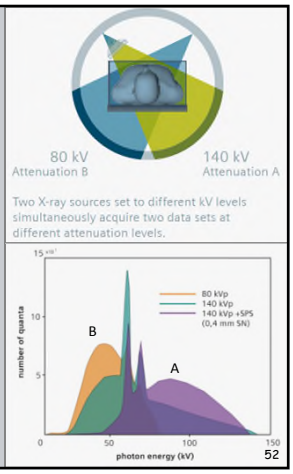

GE CT750 HD

High Speed kV switching

- 0.5 second rotation
- 0.5 ms kV switching
- Dual energy prereconstruction algorithm
- Computes:
  - Effective Z
  - Density
  - 'mono E' images

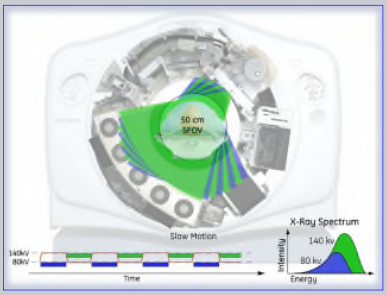

Goodsitt M et. al., Accuracies of the synthesized monochromatic CT numbers and effective atomic numbers obtained with a rapid kVp switching dual energy CT scanner, Medical Physics 38 (4), 2011.

GE CT750 HD

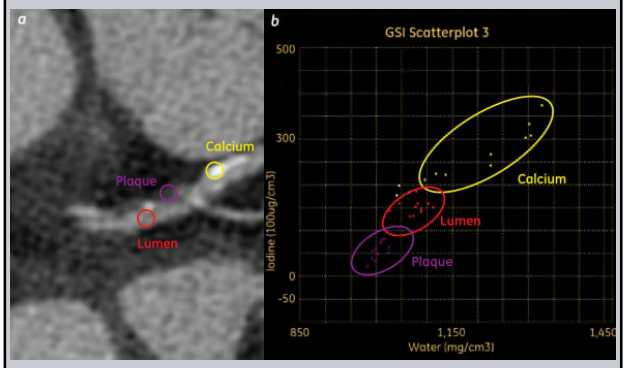

Coronary artery Dual Energy tissue identification

VII.A.6 – Recent Designs, Dual Energy

Philips IQon Spectral CT

Multi Layer Detector

- yttrium-based garnet scintillator for detection of lower energies
- gadolinium oxysulphide (GOS) scintillator for detection of higher energies
- Thin front-illuminated photodiode (FIP), which is placed vertically.
  - The photodiode lies beneath the anti-scatter grid as to not degrade the overall geometric efficiency of the detector
- Integrated application-specific integrated circuit (ASIC) for analog-to-digital conversion.

- While not ideal for DE material imaging, SE & DE is obtained at the same time.
- The detector offers potential for CNR improvement from energy weighting.

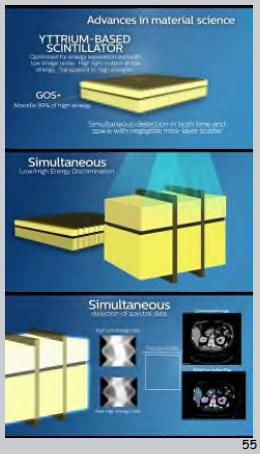

11/2014 FDA approval

VII.A.6 – Recent Designs, Inverse Geometry

Prototype system
- Stanford Univ.
- GE Global Research

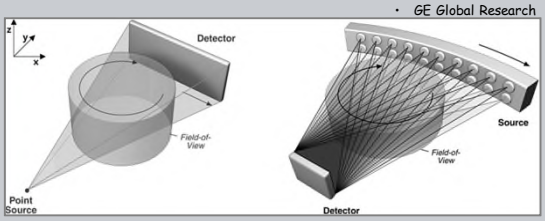

Table 1. System parameters.

Source to isocenter distance	450 mm
Detector to isocenter distance	385 mm
Source spacing in x and z	25 mm and 100 mm
Detector dimension in x and z	70 mm × 192 mm
Detector cell size in x and z	1.1 mm × 1.0 mm
FOV(axial × transverse)	75 mm × 160 mm
Source voltage	80 kVp
Source current	125 mA
Exposure time per source location per view	5.4 μs
Number of views per source	125/360°
Rotation time per revolution	1 s

Phys. Med. Biol. 59 (2014) 1189–1202

VII.A.6 – Recent Designs, Inverse Geometry

Prototype system
- Stanford Univ.
- GE Global Research

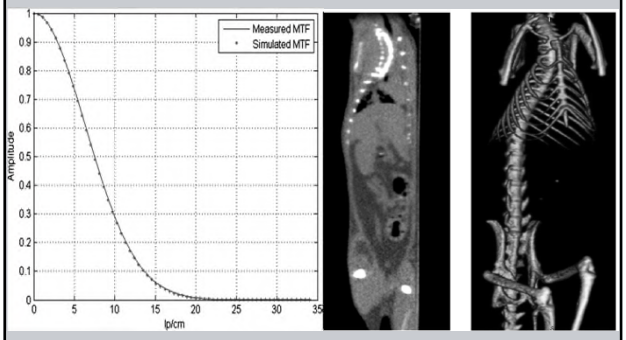

Phys. Med. Biol. 59 (2014) 1189–1202

Med. Phys. 43 (2016) part I 4604-4616

Med. Phys. 43 (2016) part II 4617-4627

VII.A.6 – Recent Designs, Photon Counting CT

Prototype system
Siemens Medical, Mayo Clinic

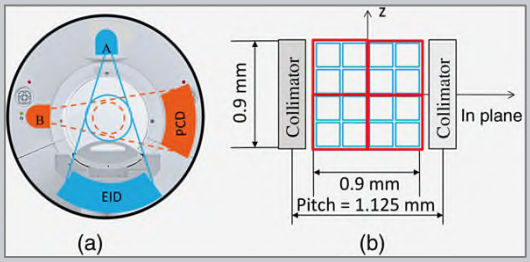

(a) A research PCD-based CT system, built based on a second-generation dual-source CT system, consists of an EID and a PCD. (b) Detector configuration of the UHR mode of the PCD, showing both native pixels (blue) and UHR pixels (red).

Yu, SPIE JMI, oct 2016

Leng, SPIE JMI, oct 2016

VII.A.6 – Recent Designs, Photon Counting CT

Prototype system
Siemens Medical, Mayo Clinic

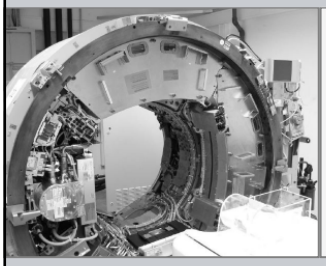

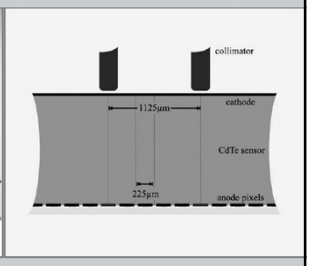

- The photon counting detector consisting of 30 modules with 128x64 quadratic sub-pixels of 225m pitch.
- Every sub-pixel features two individually adjustable energy thresholds, enabling contrast-optimization and multi-energy scans.

Kappler, SPIE MI, 2014

Leng, SPIE MI, 2015

VII.A.6 – Recent Designs, Photon Counting CT

Prototype system
Siemens Medical, Mayo Clinic

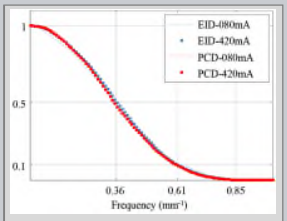

"Measurement of in-plane spatial resolution. For each subsystem, there was no noticeable difference in the measured MTF curves between 80 and 420 mA, indicating consistent in-plane spatial resolution across different tube currents."

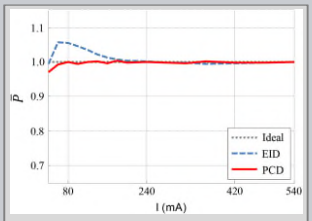

"Normalized product of noise and square root of tube current. The normalized product for the EID subsystem was >1 at low tube currents, which is evidence of electronic noise. The normalized product for the PCD subsystem was 1 for tube currents between 80 and 540 mA."

Yu, SPIE JMI, oct 2016

Prototype system
Siemens Medical, Mayo Clinic

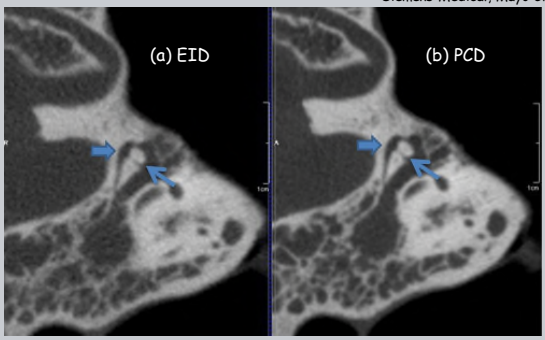

Images of the temporal bone specimen scanned with (a) EID UHR and (b) PCD UHR modes. Lower noise can be appreciated in the PCD image. The malleus head and incus body are well visualized (arrow heads).

Leng, SPIE JMI, oct 2016

Prototype system
Siemens Medical, NIH

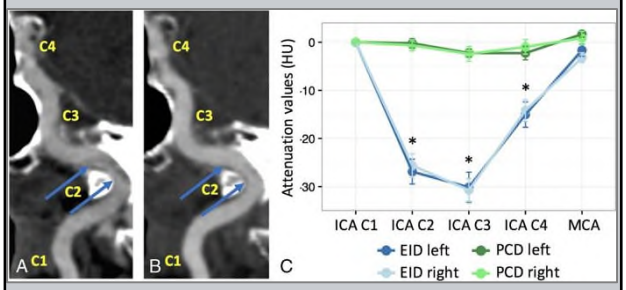

Artifactual areas of low density within the ICA petrous segment (C2) that may be mistaken for pathology are seen on the EID images but not on the PCD images (arrows).

Symons, Invest. Rad., Mar. 2018

Prototype system
Siemens Medical, Mayo Clinic

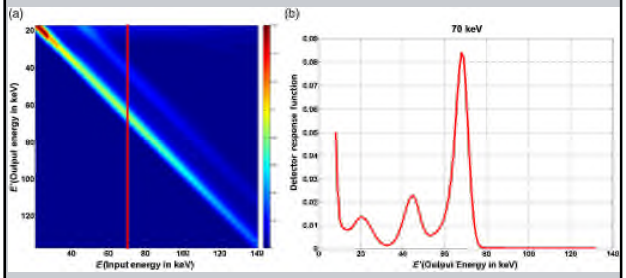

a) The two-dimensional detector response function, p(E',E), represents the probability of a photon of energy E being detected at an energy E'.

b) An example of the detector response function is shown for an incident photon of energy 70 keV.

Li, J. Med. Img., Apr. 2017

Prototype system
Siemens Medical, NIH

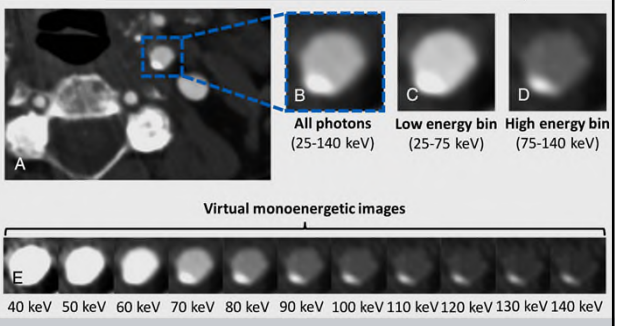

Based on the material attenuation at different photon energy levels, images can be decomposed into their constituent materials (eg, iodine versus calcium) and virtual monoenergetic images (E) can be reconstructed to enhance facilitate plaque detection.

Symons, Invest. Rad., Mar. 2018

A) X-ray Computed Tomography

1. Basic Concepts
2. Historical Developments
3. X-ray Source
4. Detectors
5. Multi-slice scanners
6. Recent Advances
7. Cone beam systems (9 slides)
8. Tomosynthesis systems

- Lee Feldkamp PhD, Ford Motor Co.
- Mike Parfitt MD, Henry Ford Health
- Steve Goldstein PhD, Univ. of MI

Feldkamp, Davis & Kress
JOSA 1984
"A convolution-backprojection formula is deduced for direct reconstruction of a three dimensional density function from a set of two-dimensional projections."

Feldkamp, Goldstein & Parfitt
J. Bone & Mineral Res. 1989
"We describe a new method for the direct examination of three-dimensional bone structure in vitro based on high-resolution computed tomography (CT)"

Cone beam mCT was developed by Lee Feldkamp (left) for industrial inspection and used by Michael Parfitt (right) to examine embedded bone specimens from the iliac crest.

VII.A.7 – mCT : specimen systems

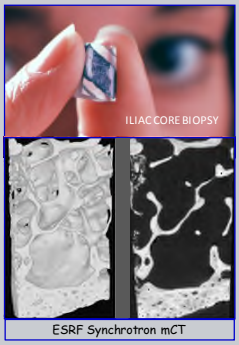

ESRF Synchrotron mCT

Cone beam mCT laboratory system (hfhs) with micro focus source (left), specimen rotation stage (Ctr.) and flat paned detector (right). Components are installed on a granite bench with tracks to adjust distances and set the geometric magnification.

VII.A.7 – Geometry nomenclature

Specimen and industrial cone beam CT system rotated the object about a single axis. The object region of interest was recorded at many angles using a single large area detector

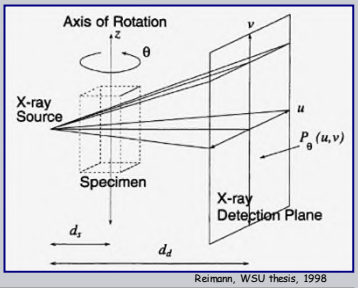

Reimann, WSU thesis, 1998

- For patients and live animals, this has been extended to keep the object stationary and rotate the detector.
- Cone beam systems use a single large detector and broad beam to record in a single axial rotation.

VII.A.7 – mCT Systems for Animal Research

- Cone beam CT systems are now commercially available for animal research in pre-clinical research studies.
- Systems use flat panel digital radiography detectors capable of acquiring images in rapid sequence (30 fps).

GE Explore Locus

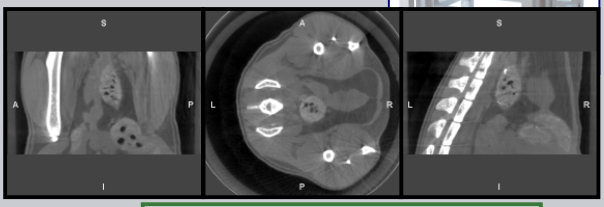

Volumetric Scan of a mouse thorax (50 micron voxel)

VII.A.7 – Dental / ENT CT systems

- Cone beam systems are now commonally used for dental implant services and Ear Noise and Throat (ENT) diagnosis.
- The Xoran miniCat system uses a flat panel CsI indirect DR detector (Varian PaxScan)

http://www.xorantech.com

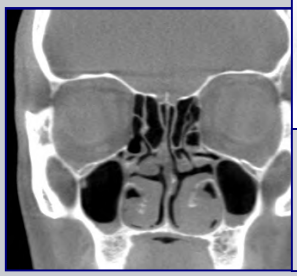

- Xoran Technologies, Inc. was founded in 2001 by two research scientists from the University of Michigan with the goal of developing common sense, innovative technologies that enable physicians to treat their patients more efficiently and more effectively.
- In the past ten years, they have installed more than 400 CT scanners domestically and internationally.

VII.A.7 – Dental / ENT CT systems

3D Dental images, Instrumentarium Dental

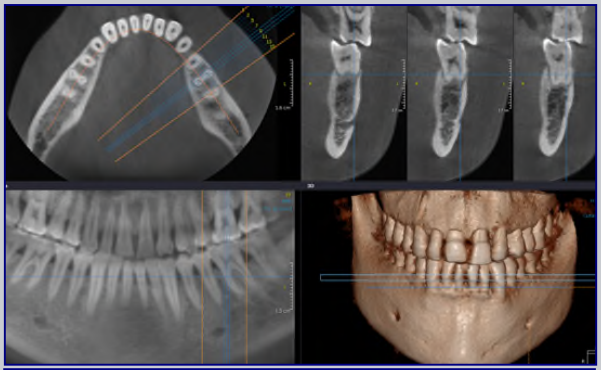

http://www.instrumentariumdental.com/france/produits/systeme-dimagerie-dentaire-3d-a-faisceau-conique.aspx

VII.A.7 – Angiography cone beam CT systems

Media link for Artis Dyna CT

Siemens Artis zeego syngo Dyna CT

Right: Robotic arms are now used to move an x-ray tube and angiographic rapid sequence detector in a circular orbit for cone beam tomography.

Left: Vessel supplying blood to a chest tumor.

VII.A.7 – Equine cone beam CT system

4DDI Equine

Helios Equimagine ™

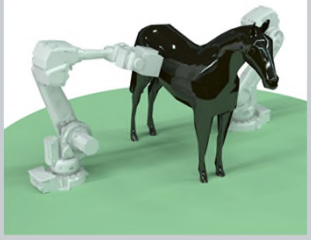

Equine Hock Joint

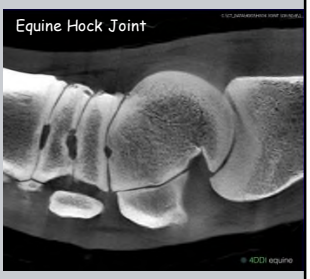

Left: Robotic x-ray system developed specifically for large animal veterinary medicine applications.

Right: cone beam CT Sagittal view of an equine hock joint.

http://equine4ddi.com/

VII.A.7 – Scatter in Cone Beam Systems

Siewerdsen JH, Jaffray DA: Cone-beam computed tomography with a flat-panel imager Magnitude and effects of x-ray scatter, Med. Phys. Feb. 2001

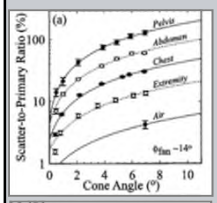

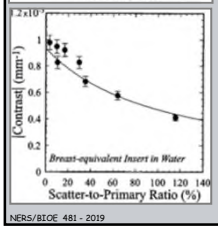

- The broad beam used in cone beam CT systems results in scatter radiation that reduces contrast in the projection views.
- The reconstructed value and the contrast of targets objects is reduced as a consequence.

$$\mu' d = \mu d + \ln\left(\frac{1}{1+S/P}\right)$$

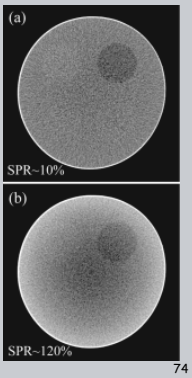

VII.A – CT outline

A) X-ray Computed Tomography

1. Basic Concepts
2. Historical Developments
3. X-ray Source
4. Detectors
5. Multi-slice scanners
6. Recent Advances
7. Cone beam systems
8. Tomosynthesis systems (10 slides)

VII.A.8 – Tomosynthesis

- Cone Beam Tomo

CB CT systems typically acquire data from large area detectors rotating in a circular orbit for a rotation angle of 360°.

- Tomosyntheses

For tomosynthesis systems, an approximate inverse solution is deduced from data obtained over a limited rotation angle.

The reconstruction has limited depth separation, but high spatial resolution.

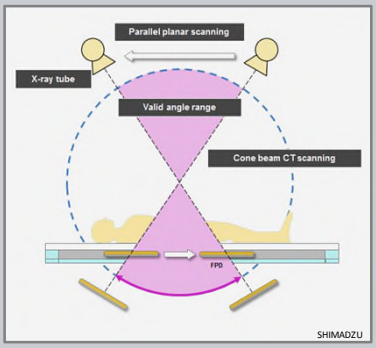

VII.A.8 – Tomosynthesis: Shimadzu Sonialvision / Safire

- The Shimadzu Sonialvision / Safire system integrates the digital detector within a radiographic tilt table.
- Shown in the tilt position for a lateral knee tomosynthesis acquisition (60°), the detector translates up and the x-ray tube moves downward.
- The x-ray central beam is directed at the joint surface with an angle that varies from -20 to +20 degrees

VII.A.8– Tomosynthesis: GE VolumeRAD

- For the GE VolumeRAD system, the tube angle changes as the tube mount moves linearly.
- The detector remains in a stationary position.

VII.A.8– Tomosynthesis: Siemens breast TS

Tomosynthesis systems designed for breast imaging have been shown to be effective for early diagnosis of breast cancer.

VII.A.8 – Tomosynthesis Reconstruction

Filtered Backprojection

- The reconstruction is similar to cone beam CT but with a limited acquisition angle.
- The tomosynthesis image quality can be understood from the Fourier representation of the acquired data.

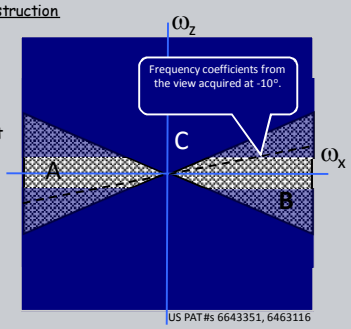

US PAT #s 6643351, 6463116

A. High signal frequencies in the x,y directions provide in-plane detail.
B. Varied filter cut-off frequencies vs angle limit Z signal resolution.
C. Flat surfaces are not sampled along the ω_z direction

VII.A.8 – Tomosynthesis : 3D spatial frequency domain

TS vs CT

Unsampled frequencies along the ω_y axis make TS and CT complimentary.

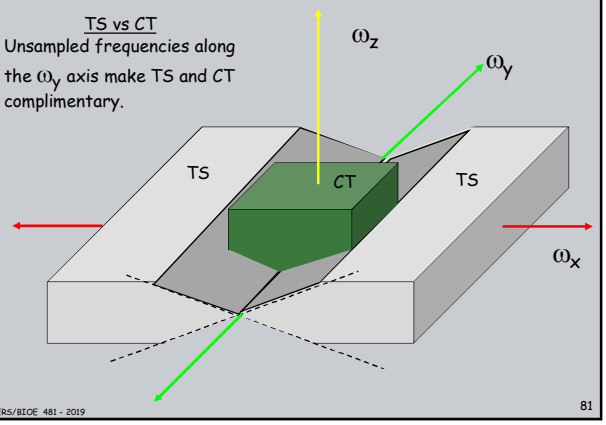

VII.A.8 – Tomosynthesis: knee AP view

Gazeille, Flynn, Page et.al.
Skeletal Radiology
07 Aug 2011 (online)

AP view obtained with toe in and hip elevated with a boomerang filter.

VII.A.8 – TS: knee AP view

TS images are in a plane through the head, neck, and shaft.

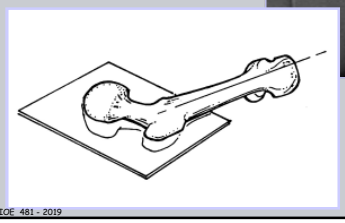

VII.A.8 – TS: Hip Trochanter fracture

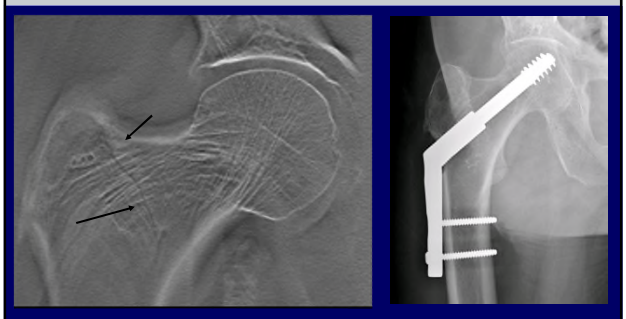

- Tomosynthesis showed a transverse fracture from thetrochanter through the base of the neck.
- The patient was sent to surgery for a hip screw.

VII.A.8– Tomosynthesis: breast TS

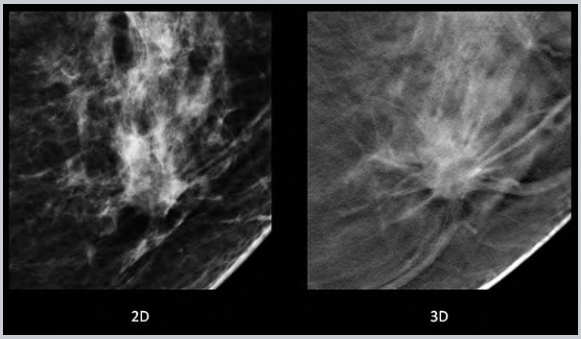

- Conventional mammogram (2D) versus breast tomosynthesis (3D).
- When used with FFDM, DBT has been shown to improve cancer detection and reduce callbacks for additional examinations.

L11 – CT, part A

?